THE JOURNAL OF BIOLOGICAL CHEMISTRY VOL. 288, NO. 25, pp. 18172–18183, June 21, 2013

Endoplasmic Reticulum Stress Regulates Rat Mandibular Cartilage Thinning under Compressive Mechanical Stress*[S]

Received for publication, February 1, 2013, and in revised form, April 12, 2013 Published, JBC Papers in Press, April 19, 2013, DOI 10.1074/jbc.M112.407296

Huang Li[‡1], Xiang-Yu Zhang[‡], Tuo-Jiang Wu[§], Wei Cheng[‡], Xin Liu[‡], Ting-Ting Jiang[‡], Juan Wen[‡], Jie Li[‡], Qiao-Ling Ma[‡], and Zi-Chun Hua[‡2]

From the [‡]School of Stomatology and State Key Laboratory of Pharmaceutical Biotechnology, Nanjing University, 30 Zhongyang Road, Nanjing 210009, China and the [§]Stomatological College of Nanjing Medical University, Nanjing 210029, China

Background: The molecular mechanisms of mechanical stress-induced cartilage thinning remain largely unknown.
Results: Endoplasmic reticulum stress (ERS) was activated in chondrocytes during mechanical stress loading. ERS inhibition suppressed the apoptosis and restored the proliferation and cartilage thinning.
Conclusion: ERS regulates mechanical stress-induced cartilage thinning.
Significance: Our data demonstrate a novel pathological role for ERS and provide new insight into the treatment of temporomandibular joint diseases.

Compressive mechanical stress-induced cartilage thinning has been characterized as a key step in the progression of temporomandibular joint diseases, such as osteoarthritis. However, the regulatory mechanisms underlying this loss have not been thoroughly studied. Here, we used an established animal model for loading compressive mechanical stress to induce cartilage thinning *in vivo*. The mechanically stressed mandibular chondrocytes were then isolated to screen potential candidates using a proteomics approach. A total of 28 proteins were identified that were directly or indirectly associated with endoplasmic reticulum stress, including protein disulfide-isomerase, calreticulin, translationally controlled tumor protein, and peptidyl-prolyl *cis*/*trans*-isomerase protein. The altered expression of these candidates was validated at both the mRNA and protein levels. The induction of endoplasmic reticulum stress by mechanical stress loading was confirmed by the activation of endoplasmic reticulum stress markers, the elevation of the cytoplasmic Ca^{2+} level, and the expansion of endoplasmic reticulum membranes. More importantly, the use of a selective inhibitor to block endoplasmic reticulum stress *in vivo* reduced the apoptosis observed at the early stages of mechanical stress loading and inhibited the proliferation observed at the later stages of mechanical stress loading. Accordingly, the use of the inhibitor significantly restored cartilage thinning. Taken together, these results demonstrated that endoplasmic reticulum stress is significantly activated in mechanical stress-induced mandibular cartilage thinning and, more importantly, that endoplasmic reticulum stress inhibition alleviates this loss, suggesting a novel pharmaceutical strategy for the treatment of mechanical stress-induced temporomandibular joint diseases.

The temporomandibular joint (TMJ)[3] is a unique joint in the body; it is composed of stress-sensitive cartilage that is subject to extensive tissue remodeling (1). During orthodontic treatment, mechanical loading plays a pivotal role in the remodeling of mandibular cartilage and influences the growth of the mandible in the treatment of Class III malocclusion (mandibular prognathism) (2). Furthermore, various studies have shown that repeated increases in mechanical stress are closely associated with TMJ osteoarthritis. Cartilage thinning as a result of excessive mechanical stress has been recognized as a major factor in the development of TMJ osteoarthritis (3–5).

Mechanotransduction is the process of transmitting mechanical stimulation to cells. Previous studies have indicated that chondrocytes receive mechanical signals and integrate these signals with those from other signaling molecules, such as hormones and growth factors, thus determining cell fate. Several signaling pathways in chondrocytes are activated by mechanical stress (*e.g.* interleukin-4 (cytokine) signaling (6), intracellular calcium changes (7), and p38 MAPK phosphorylation (8)). However, the molecular mechanisms involved in cartilage thinning remain poorly understood.

Proteomic analysis provides a comprehensive view of cellular responses to various stimuli. This approach has been successfully utilized to examine chondrocyte differentiation and cartilage pathophysiology (9, 10). Our previous study of the response of mandibular chondrocytes to mechanical stress *in vitro* demonstrated a transient but inhibitory effect on cell cycle progression, accompanied by cytoskeleton remodeling and MAPK pathway activation (11). However, the molecular mechanisms regulating mandibular cartilage responses to mechanical stress *in vivo* have not been thoroughly investigated, and the determinants mediating cartilage loss induced through mechanical stress remain largely unknown.

* This work was supported by the National Natural Science Foundation of China and Nanjing Medical Science and Technique Development Foundation Contract Grants 81070807, 81200764, 81121062, and 50973046.
[S] This article contains supplemental Table S1 and Figs. S1–S4.
[1] To whom correspondence may be addressed. Tel.: 86-025-83620173; Fax: 86-025-83620173; E-mail: Lihuang76@nju.edu.cn.
[2] To whom correspondence may be addressed. Tel.: 86-025-83620173; Fax: 86-025-83620173; E-mail: zchua@nju.edu.cn.

[3] The abbreviations used are: TMJ, temporomandibular joint; CRT, calreticulin; HSP, heat shock protein; PCNA, proliferating cell nuclear antigen; PDI, protein-disulfide isomerase; TCTP, translationally controlled tumor protein; TEM, transmission electron microscopy; WB, Western blot; ERS, endoplasmic reticulum stress.

Here, we used an established rat model to load compressive mechanical stress on mandibular cartilage. The stressed chondrocytes were then isolated for a proteomic analysis. Proteins involved in endoplasmic reticulum stress (ERS), such as protein-disulfide isomerase (PDI), calreticulin (CRT), translationally controlled tumor protein (TCTP), and Pin-1 (peptidyl-prolyl *cis*/*trans* isomerase NIMA-interacting 1), were identified. As expected, the activation of ERS occurred during the mechanical stress loading. Furthermore, significant apoptosis was observed at 3 days post-stress, whereas the inhibition of cell cycle arrest and cartilage proliferation was observed later. Moreover, the inhibition of ERS reduced the observed apoptosis at the early stages of mechanical stress loading and restored the proliferation at the later stages. The results of this study provide new insight into the role of ERS in regulating cartilage thinning under conditions of mechanical stress and might facilitate the identification of new therapeutic targets for treating TMJ diseases.

EXPERIMENTAL PROCEDURES

Compressive Mechanical Stress Loading on Rat Mandibular Cartilage—All animals were housed in an approved facility at Nanjing University. The animal use protocol followed institutional guidelines. Eight-week-old male Sprague-Dawley rats were used in this study. Compressive forces were loaded onto the TMJ as described previously (14) (see Fig. 1*A*). A rubber band was tied between the jig and the anchorage hooks to load 40 *g* of force on each side. Eight rats in each group wore the appliance for 3, 7, 14, or 21 days, with gender- and age-matched controls. None of the rats displayed signs of disability, and all animals received the same standardized diet throughout the procedure. To show the direction of mechanical stress loading, x-ray images were obtained for the control and experimental groups (30 kV, 3 mA, 1 min) (Fig. 1*A*).

Histological Observation and Histomorphometric Measurement—Rats were sacrificed by cervical dislocation under anesthesia. The TMJ was removed and fixed in 4% paraformaldehyde for 24 h. The specimens were decalcified in 15% EDTA solution for 8 weeks and embedded in paraffin after thorough rinsing. Sagittal sections 4 μm in thickness were cut. The histological changes in mandibular cartilage were examined by hematoxylin-eosin (H&E) staining. Two sets of five stained sections from each experimental period were used for histomorphometric analysis. The entire mandibular cartilage area was divided into three zones (fibrous proliferation (*FP*), transition (*T*), and hypertrophic zones (*H*)) from the *top* to the *bottom* (Fig. 1*B*). This regionalization method has been extensively used in studies on mandibular condylar cartilage (12–15). The thickness of each zone was measured with Image-Pro Plus software.

The 14-day experimental group and their age-matched controls were further examined using Alcian blue staining and type II collagen (1:100; rabbit anti-rat polyclonal antibody, KeyGen Biotech, Nanjing, China) immunohistochemical staining. The samples for the immunostaining of type II collagen were pretreated with hyaluronidase for 1 h.

Mandibular Condylar Chondrocyte Culture—Mandibular cartilage was obtained from Sprague-Dawley rats in the control and the experimental (14 days) groups and carefully dissected under a microscope. The dissected line is shown in *black* in Fig. 2*A*. The soft tissues of the mandibular condyle were separated using ophthalmic forceps and digested with 0.25% trypsin for 30 min. The mandibular condyle was subsequently minced and digested with 0.2% collagenase for 120 min. The primary mandibular chondrocytes were rinsed three times and prepared as a single-cell suspension in growth medium containing DMEM supplemented with 15% fetal calf serum and penicillin/streptomycin (Invitrogen). Cells were counted with a hemocytometer, and cell viability was verified with trypan blue solution. Subsequently, the cells were seeded overnight at high density ($1 \times 10^6/cm^2$) in a humidified atmosphere at 37 °C and 5% CO_2. Primary mandibular chondrocytes were examined by inverted phase-contrast microscopy. The chondrocytes were evaluated by H&E staining and validated by type II collagen (1:200; rabbit anti-rat polyclonal antibody, KeyGen Biotech) immunohistochemistry following standard procedures. The chondrocytes were cultured 3 days to reach confluence.

Isolation of Total Proteins and Phosphoproteins—The cell pellets were lysed in a cell lysis solution containing 7 M urea, 2 M thiourea, 40 mM DTT, and 2% immobilized pH gradient buffer (pH 3–10 (Linear); GE Healthcare). The lysates were sonicated in short bursts to disrupt the nucleic acids and clarified by centrifugation at 40,000 $\times$ *g* at 4 °C for 60 min to obtain total proteins. The protein concentration in the supernatant was determined using the Bradford method. Phosphoproteins were isolated from mandibular chondrocytes using the phosphoprotein purification kit (Qiagen, Hilden, Germany) as recommended by the manufacturer (16). Briefly, 1×10^7 cells were lysed in a cell lysis buffer containing detergent, nucleases, and protease inhibitors. Lysates were cleared by centrifugation at 40,000 $\times$ *g* at 15 °C for 90 min, and the supernatants were loaded onto phosphoprotein-specific columns for affinity chromatography. The eluted proteins were concentrated using Nanosep ultrafiltration columns (Pall, Dreeich, Germany).

Two-dimensional Gel Electrophoresis and MALDI-TOF MS—The protein lysates (120 μg of total protein lysates and 80 μg of the phosphoprotein fraction) were subjected to isoelectric focusing on a gel strip with a linear pH 3–10 gradient and resolved on an SDS-polyacrylamide gel. The separated proteins were visualized by diamine silver staining as described previously (17). After destaining with double-distilled water, the gels were scanned at 600 dpi resolution, and the images were processed with Adobe Photoshop software (Adobe Systems) and analyzed with Image Master Platinum™ software (GE Healthcare) according to the manufacturer's instructions. A greater than 2-fold change in the protein concentration was considered significant ($p < 0.01$; Mann-Whitney test). The differentially expressed proteins were extracted from the gel and digested as described previously (18).

MALDI samples were prepared according to a method described previously (19). Mass spectra were recorded with an Ultraflex II MALDI-TOF-TOF mass spectrometer (Bruker Daltonics GmbH, Bremen, Germany) with FlexControl™ version 3.0 software (Bruker Daltonics GmbH). The MALDI-TOF spectra were recorded in the positive ion reflector mode in a mass range of 700 – 4000 Da, and the ion acceleration voltage

was 25 kV. The acquired mass spectra were processed with FlexAnalysis™ version 3.0 software (Bruker Daltonics GmbH) with the following internal standards: peak detection algorithm, SNAP (sort, neaten, assign, and place); S/N threshold, 3; quality factor threshold, 50. The tryptic autodigestion ion picks (trypsin_[108–115], MH+842.509, trypsin_[58–77], MH+2211.104) were used as internal standards. Matrix and/or autoproteolytic trypsin fragments or known contaminant ions (keratins) were excluded. The resulting peptide masses were used to search NCBInr 20101105 (101,942 sequences) with Mascot (version 2.3.02) in automated mode, using the following criteria as search parameters: significant protein MOWSE score at $p < 0.05$, minimum mass accuracy of 120 ppm, trypsin as an enzyme, one missed cleavage site allowed, alkylation of cysteine by carbamidomethylation as a fixed modification, and oxidation of methionine as a variable modification. In addition, the Mascot score and expectation of the first non-homologous protein to the highest ranked hit were verified.

Isolation of Total RNA, RT-PCR, and Real-time Quantitative PCR—Total RNA was isolated from the control and stressed chondrocytes with the RNA simple Total RNA kit (Tiangen Biotech, Beijing, China), and reverse transcription was performed with the QuantScript RT kit (Tiangen Biotech) according to the manufacturer's instructions. cDNA was stored at −20 °C. The following primer sequences were used to generate the products: CRT, forward (GAAATGGTGCTGGTCCTTCTTCAC) and reverse (GTCACATGACACTCTCCACCACGA); TCTP, forward (ATTAGATATCCCCCCTCCCCCCGCGCGCC) and reverse (CAGTGGATCCTTAACATTTCTCCATCTCTAAGCCATC); PDI, forward (CTACGATGGCAAATTGAGCA) and reverse (CTTCCACCTCATTGGCTGTT); Pin-1, forward (TGCCCAGGCTTTTGTCAAAC) and reverse (CTCCAGTGCCAAGGTCTGAA); β-actin, forward (TCAGGTCATCACTATCGGCAAT) and reverse (AAAGAAAGGGTGTAAAACGCA). The PCR products were separated on a 1.5% agarose gel, and the expression of CRT, Pin-1, PDI, and TCTP was evaluated with Image-Pro Plus software (Media Cybernetics, Silver Spring, MD). For quantification, the mRNA expression of the above genes was normalized to that of the housekeeping gene β-actin.

For real-time quantitative PCR, the following primer sequences were used for the targeted genes: collagen II, forward (AGAGCGGAGACTACTGGATTG) and reverse (TCTGGACGTTAGCGGTGTT); collagen X, forward (TCTGGGATGCCTCTTGTC) and reverse (TCTTGGGTCATAGTGCTG); *RUNX2*, forward (CCGTGGCCTTCAAGGTTGTA) and reverse (ATTTCGTAGCTCGGCAGAGTAGTT); *OP* (osteopontin), forward (GACGGCCGAAGGTGATAGCTT) and reverse (CATGGCTGGTCTTCCCGTTG); *FSP1*, forward (AGCTACTGACCAGGGAGCTG) and reverse (TGCAGGACAGGAAGACACAG); vimentin, forward (GCACCCTGCAGTCATTCAGA) and reverse (GCAAGGATTCCACTTTACGTTCA); β-actin, forward (GAGACCTTCAACACCCCAGC) and reverse (ATGTCACGCACGATTTCCC). All genes were analyzed using an Applied Biosystems 7500 real-time PCR machine. Each experiment was performed three times, and the mean values were calculated. The amount of target cDNA relative to β-actin was calculated using the formula $2^{-\Delta\Delta}C_t$. The results were calculated as the relative quantification of the target gene compared with the control group.

Western Blot Analysis—Total proteins were extracted from the control and stressed chondrocytes and quantified as described above. A total of 25 μg of total proteins/lane was loaded and separated on a 12% SDS-polyacrylamide gel. The proteins were transferred to Immobilon-P membranes (PVDF; Millipore Corp., Billerica, MA). The membranes were incubated for 2 h with antibodies, including rabbit polyclonal anti-calreticulin (1:500) and mouse monoclonal anti-TCTP (1:250) (Abcam); rabbit polyclonal anti-phospho-Pin-1 (1:500), rabbit polyclonal anti-PDI (1:1000), mouse monoclonal anti-CHOP (1:1000), rabbit polyclonal anti-phospho-eIF2α (1:1000), and rabbit polyclonal anti-cleaved caspase-3 (1:1000) (Cell Signaling Technology); rabbit polyclonal anti-cyclin D1 (1:1000) (BD Pharmingen); rabbit polyclonal anti-Bip (1:1000) (Epitomics Inc.); and rabbit polyclonal anti-α-tubulin (Santa Cruz Biotechnology, Inc., Santa Cruz, CA) (1:2000), followed by incubation with anti-mouse, anti-rabbit, or anti-goat HRP-conjugated secondary mAbs (Santa Cruz Biotechnology, Inc.) (1:5000) for 1 h. The membranes were visualized using an ECL Plus kit (Amersham Biosciences) and quantified by densitometry.

Immunohistochemical Staining—Changes in the expression of PDI, CRT, phospho-Pin-1, TCTP, cyclin D1, PCNA, and Ki67 were observed by immunochemistry. The sections were rinsed with PBS. The antigens were retrieved by using an enzyme mixture containing trypsin and pepsin for 1 h at 37 °C or by heating in a pressure cooker, rinsed with PBS buffer, treated with 3% H_2O_2 in PBS, rinsed again with PBS, incubated with 10% normal rabbit or goat serum at room temperature for 10 min, and treated with one of nine antibodies, including CRT (1:100), TCTP (1:250), phospho-Pin-1 (1:50), PDI (1:100), cyclin D1 (1:100), rabbit polyclonal anti-Ki67 (1:100) (Abcam), and goat polyclonal anti-PCNA (1:100) (Zhongshan Inc.), in a moist chamber overnight at 4 °C. After incubation with secondary IgG antibodies (HRP-conjugated) for 30 min at 37 °C, the sections were rinsed and incubated for 30 min with SP complex at 37 °C. The samples were stained with diaminobenzidine (SP immunochemistry kit, Boster Biological Technology, Ltd., Wuhan, China). The cell nuclei were counterstained with hematoxylin. The stained samples were embedded on microscope slides with neutral resins. A color difference was used to delineate positive and negative areas, which were measured with Image-Pro Plus software.

Flow Cytometry Analysis—Chondrocytes from the control and experimental groups (14 days) were fixed in 75% ice-cold ethanol and incubated with RNase A (200 mg/ml) in PBS at 37 °C for 30 min. The fixed cells were subsequently washed twice with PBS, stained with propidium iodide in PBS, and analyzed by flow cytometry (BD Biosciences). The distribution of the cells in different cell cycle phases was indicated by the cellular DNA content profiles. A minimum of 10,000 events were counted for each sample. To detect apoptosis, annexin V and propidium iodide staining were performed using the annexin V-FITC/propidium iodide apoptosis kit (Biovision). The chondrocytes from the control and experimental groups were washed, trypsinized, and pelleted. The supernatant was removed, and the cells were resuspended in staining buffer con-

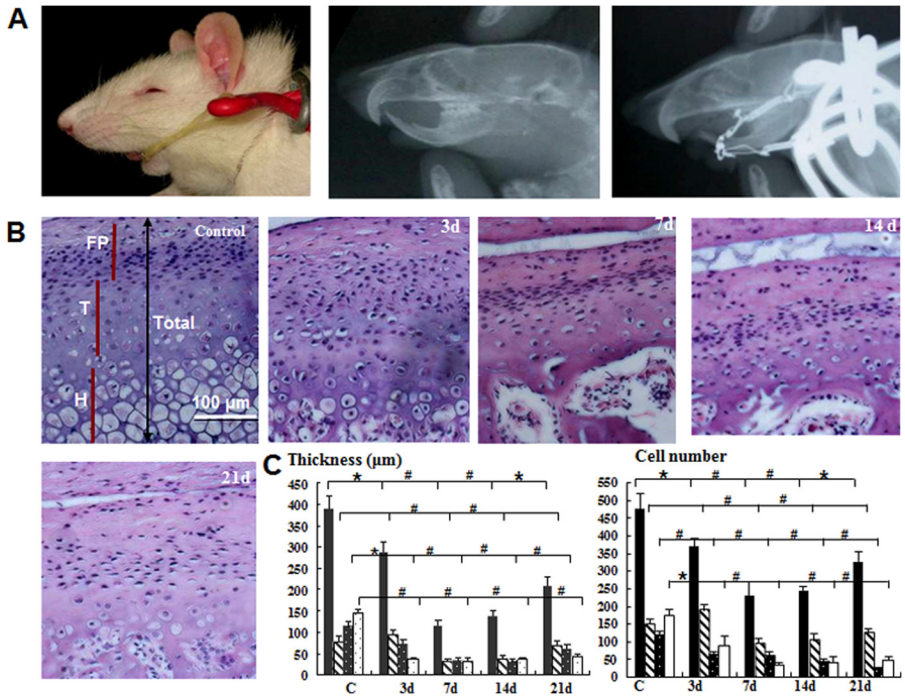

FIGURE 1. **Compressive mechanical stress induces mandibular cartilage thinning.** *A*, an appliance that loaded 40 *g* of force on each side was used to move the mandible posteriorly and superiorly. *B*, H&E staining (magnification ×100) of samples subjected or not subjected to mechanical stress for the number of days indicated. *P*, proliferative zone; *T*, transition zone; *H*, hypertrophic zone. *C*, quantitative analysis of cartilage thickness and the cell number from the samples shown in *B* (*, $p < 0.05$; #, $p < 0.01$). *Error bars*, S.D.

taining the annexin V-FITC antibody and propidium iodide. The cells were analyzed by flow cytometry (FACSCalibur, BD Biosciences) with CellQuest software version 3.3 (BD Biosciences).

TUNEL Staining—Tissue sections (4 μm in thickness) were prepared according to standard protocols for H&E staining. The apoptotic cells in each section (three sections per rat, eight rats in each group) were visualized using terminal deoxynucleotidyltransferase-mediated dUTP nick end labeling (TUNEL) according to the manufacturer's instructions (Boster Biological Technology, Ltd.).

Determination of Free Ca^{2+} in Chondrocytes—Free Ca^{2+} was measured in chondrocytes as described previously (20). Briefly, the chondrocytes were incubated with Fluo-AM (GenMed) according to the manufacturer's recommendations and visualized by immunofluorescence microscopy (Olympus). The mean fluorescence intensity was used to evaluate the relative level of cytoplasmic free Ca^{2+} and calibrated to 1.0 in the control group.

ERS Inhibitor Injection in TMJ—A total of 40 8-week-old Sprague-Dawley rats were organized into four groups: control, mechanically stressed, control plus ERS inhibitor injection, and mechanically stressed plus ERS inhibitor injection. Salubrinal (Calbiochem) was dissolved in dimethyl sulfoxide and further diluted with saline. The anesthetized rats were given injections of salubrinal (15 μl, 75 μM solution) (21) into the articular capsules of the condyle (22) 30 min before compressive stress loading, and the injections were repeated every other day. After 14 days, the rats were sacrificed as described previously. Histological changes were observed using H&E staining, and the ultrastructure changes were determined by transmission electron microscopy (TEM). PCNA and Ki67 immunochemical staining were used to detect proliferation changes in the mandibular cartilage. The changes in apoptosis were observed using TUNEL staining after 3 days of mechanical stress loading.

Statistical Analysis— All experiments were repeated three times. The data were expressed as the means ± S.D. and compared using a *t* test or analysis of variance, depending on whether the data were normally distributed. All statistical analysis was performed with SPSS version 11.0 software, and $p < 0.05$ was considered statistically significant.

RESULTS

Thinning of Mandibular Cartilage under Compressive Mechanical Stress Conditions and in Vitro Culture of Mechanically Stressed Chondrocytes—To explore the mechanisms involved in cartilage thinning *in vivo*, we used an established animal model for mechanical stress loading on mandibular cartilage. The efficiency of the model was verified by x-ray analysis, which demonstrated that the mandible moved posteriorly and superiorly, similar to clinical observations (Fig. 1*A*, *top*). The H&E staining analysis showed that the chondrocytes in the mandibular cartilage appeared disordered and disarranged at 3 days compared with the controls, whereas the thickness of the transitional and hypertrophic zones appeared slightly reduced (Fig. 1, *B* and *C*, and supplemental Fig. S1*A*). At 7 and 14 days, the thickness of the cartilage and the numbers of chondrocytes were reduced significantly in all regions (Fig. 1, *B* and *C*, and supplemental Fig. S1*A*). In the 14-day experimental group, the thinning mandibular cartilage was almost one-third the thickness of the control cartilage, and the cell number was approximately one-half the cell number of the control group. At 21

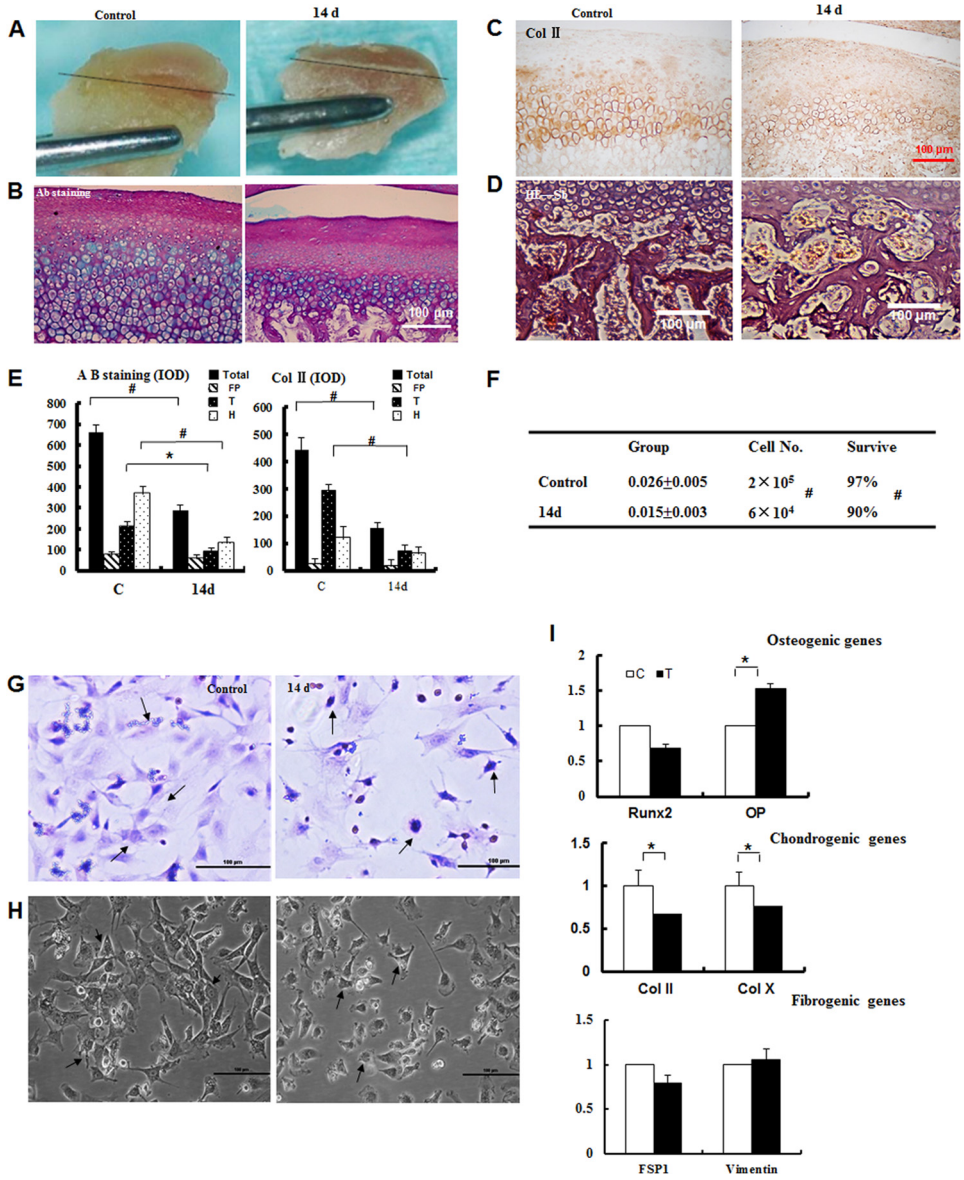

FIGURE 2. **Isolation and characterization of mechanically stressed chondrocytes.** *A*, chondrocytes were isolated from the covered cartilage (*above black lines*) in control and 14-day samples. *B*, the cartilage was untreated or treated for 14 days, and the samples were subsequently stained with Alcian blue (*Ab*) (magnification ×100). *C*, the samples from *C* were subjected to collagen II (*Col II*) immunostaining. *D*, expansion of the bone marrow space and subchondral bone erosion were observed (magnification ×100). *E*, the quantitative analysis from *B* and *C* confirmed the observations in the extracellular matrix and the loss of collagen II immunostaining. *, $p < 0.05$; #, $p < 0.01$. *F*, the cell numbers and the survival rate were reduced in the 14-day group (#, $p < 0.01$). *G*, the primary chondrocyte cultures were evaluated by H&E staining (magnification ×100). *H*, the primary chondrocytes cultures were examined by inverted phase-contrast microscopy (magnification ×100). *I*, real-time quantitative PCR analysis of osteogenic, chondrogenic, and fibrogenic genes as indicated. *Error bars*, S.D.

days, the thickness of each zone appeared to have increased slightly (Fig. 1, *B* and *C*, and supplemental Fig. S1*A*). These results demonstrated that compressive mechanical stress reduces the number of chondrocytes and the thickness of mandibular cartilage and results in mandibular cartilage thinning.

Next, we chose the 14-day loading time point to study the changes in the mandibular cartilage in further detail. The cartilage in the control group appeared transparent, shiny, and elastic, whereas the cartilage in the experimental group appeared dry, dark, and lacking in elasticity, with reduced thickness and increased bone sclerosis (Fig. 2*A*). Alcian blue staining confirmed the changes in the thinning cartilage and revealed a reduction in the amount of extracellular matrix (Fig. 2, *B* and *E*). Furthermore, the strong collagen II immunostaining was lost in the experimental group (Fig. 2, *C* and *E*). Expanded bone marrow space and trabecular changes were observed (Fig. 2*D*), indicating the erosion of the mandibular subchondral bone. *In vitro*, the weight of the mandibular cartilage was reduced from 0.026 ± 0.005 μg to 0.015 ± 0.003 μg (Fig. 2*F*).

To further explore the cellular responses of chondrocytes to mechanical stress, we isolated chondrocytes and performed H&E staining and collagen II immunostaining. The primary mandibular condylar chondrocytes in the control group were polygon-shaped and exhibited the typical characteristics of chondrocytes. In the experimental group, the numbers of chondrocytes were reduced to one-third the number of the control group (Fig. 2*F*). Although the size and shape of the chondro-

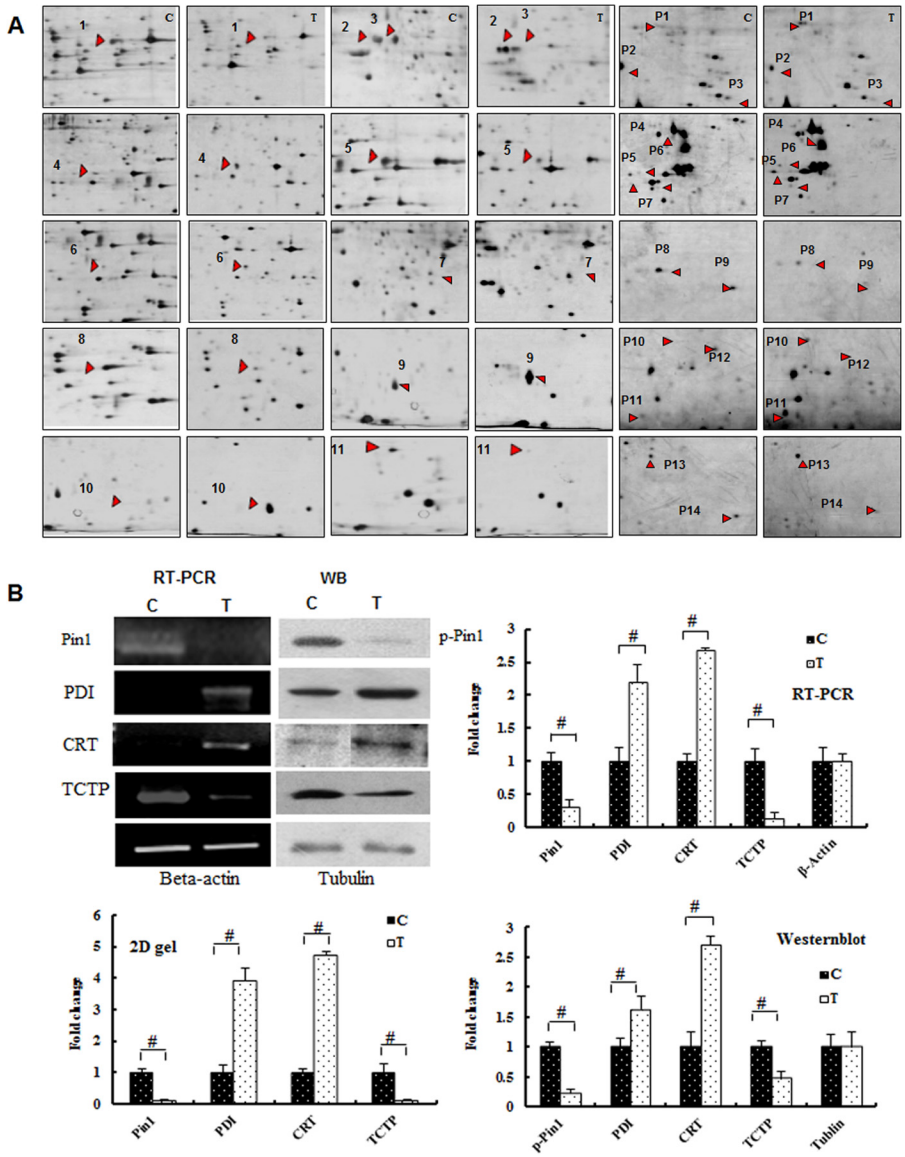

FIGURE 3. **Identification of differentially expressed proteins by proteomic analysis.** *A*, the protein spots are indicated with *arrows* and *numbers* corresponding to the proteins listed in supplemental Table 1. *B*, RT-PCR and Western blot (*WB*) analyses of the proteins, as indicated, and quantification of the -fold changes observed in the two-dimensional gel, RT-PCR, and Western blot analyses of these proteins (#, $p < 0.01$). *Error bars*, S.D.

cytes changed (Fig. 2, *G* and *H*), collagen II immunostaining was detected in both groups (supplemental Fig. S1*B*).

To examine whether mechanical stress promotes the differentiation of chondrocytes, we determined the mRNA levels of different marker molecules, such as the chondrogenic genes type II collagen and type X collagen, the fibrogenic genes FSP1 and vimentin, and the osteogenic genes *RUNX2* and *OP* (Fig. 2*I*). There was almost no significant change in the expression of *FSP1* and vimentin, and the expression of type II and type X collagen decreased. These results suggest that the compressive force in our model had insignificant effects on fibroblasts, whereas reductions in chondrogenic cells were observed. Interestingly, the reduced expression of *RUNX2* and increased *OP* mRNA suggested high metabolic activity and enhanced subchondral bone sclerosis.

Identification of Differentially Expressed Proteins by Proteomic Analysis—A proteomic analysis of the isolated chondrocytes was performed (Figs. 2*B* and 3*A* and supplemental Fig. S2) to identify the proteins responsive to compressive mechanical stimuli. The two-dimensional electrophoresis gels of whole proteins displayed 1867 ± 61 protein spots and 1588 ± 96 protein spots in each group (*i.e.* 3–12 and 14–195 kDa, respectively), and the phosphoproteins gels displayed 472 ± 32 and 454 ± 48 proteins spots, respectively. The image analysis revealed that mechanical stress modified the expression of 72 spots in the protein gels and 36 spots in the phosphoprotein gels, of which 25 significantly changed proteins ($p < 0.01$) were identified by mass spectrometry (supplemental Table S1).

The bioinformatics analysis (data not shown) identified interesting proteins that are directly or indirectly related to ERS. For example, ER molecular chaperones, such as PDI, CRT, and reticulocalbin-1, were highly expressed during ERS. The ER-resident protein Pin-1 and the Ca^{2+}-binding protein TCTP were down-regulated in response to ERS. Thus, these data suggest that ERS occurs in chondrocytes under compressive mechanical stress.

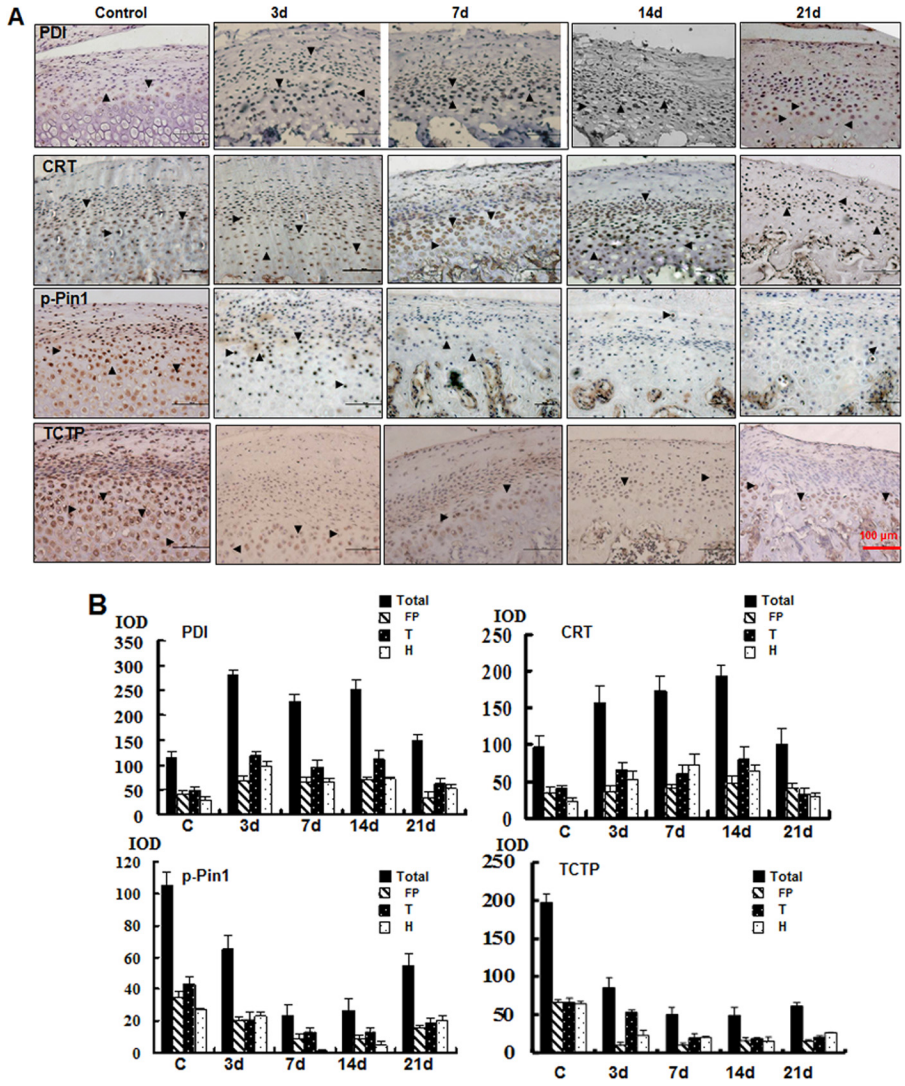

FIGURE 4. **Immunohistochemical analysis of time-dependent changes in the differential expression of proteins *in vivo*.** *A*, immunohistochemical analysis of the proteins from samples treated for different numbers of days as indicated (magnification ×100). *B*, quantification of the changes in the expression of these proteins. The integral optical density (*IOD*) was analyzed by Image-Pro Plus. *Error bars*, S.D.

To confirm the proteomics data, we examined the expression of PDI, CRT, TCTP, Pin-1, and phospho-Pin-1 (Fig. 3*B*). The expression of phospho-Pin-1 and TCTP was dramatically reduced ($p < 0.01$), whereas the expression of PDI and CRT was increased after mechanical stress treatment ($p < 0.01$). The results of the RT-PCR and Western blot analysis indicated similar alterations in the proteomic analysis of these proteins.

Time-dependent Changes in Differentially Expressed Proteins in Vivo—We next analyzed the histological sections of mandibular cartilage using *in situ* immunohistochemistry (Fig. 4, *A* and *B*, and supplemental Fig. S3, *A* and *C*). PDI expression increased rapidly at 3 days, maintained a high level of expression at 14 days, and recovered by day 21. The expression of CRT was similar, but the response was later compared with PDI. CRT expression peaked at 14 days. The increased expression of PDI and CRT was significant in the transitional and hypertrophic zone. The expression of phospho-Pin-1 was reduced by half at 3 days, reached its lowest level at 7 days, stabilized at 14 days, and recovered at 21 days. The expression of phospho-Pin-1 was gradually reduced in the proliferative and transitional zones at 3 days but declined sharply in the hypertrophic zone at 7 days. A remarkable reduction in TCTP protein levels was observed in samples at 3 days post-treatment in the proliferative zone and remained at low levels at 21 days post-treatment. These results strongly suggest that ERS is induced by compressive mechanical stress in chondrocytes.

ERS Is Activated in Response to Mechanical Stress—To confirm the onset of ERS during mechanical stress loading, we detected the levels of established ERS-associated markers (23, 24). Bip/GRP78, phospho-eIF2α, and CHOP were up-regulated in the mechanical stress-treated samples compared with the controls. Accordingly, procaspase-3 levels were reduced, indicating that caspase-3 cleavage and activation occur in mechanically stressed chondrocytes (Fig. 5, *A* and *B*).

Increased cytoplasmic calcium distribution has been observed during ERS (24). Therefore, we determined the cytoplasmic Ca^{2+} levels in mechanical stress-treated chondrocytes (Fig. 5, *C* and *E*). As expected, the cytoplasmic Ca^{2+} levels were significantly elevated after mechanical stress treatment ($p < 0.01$).

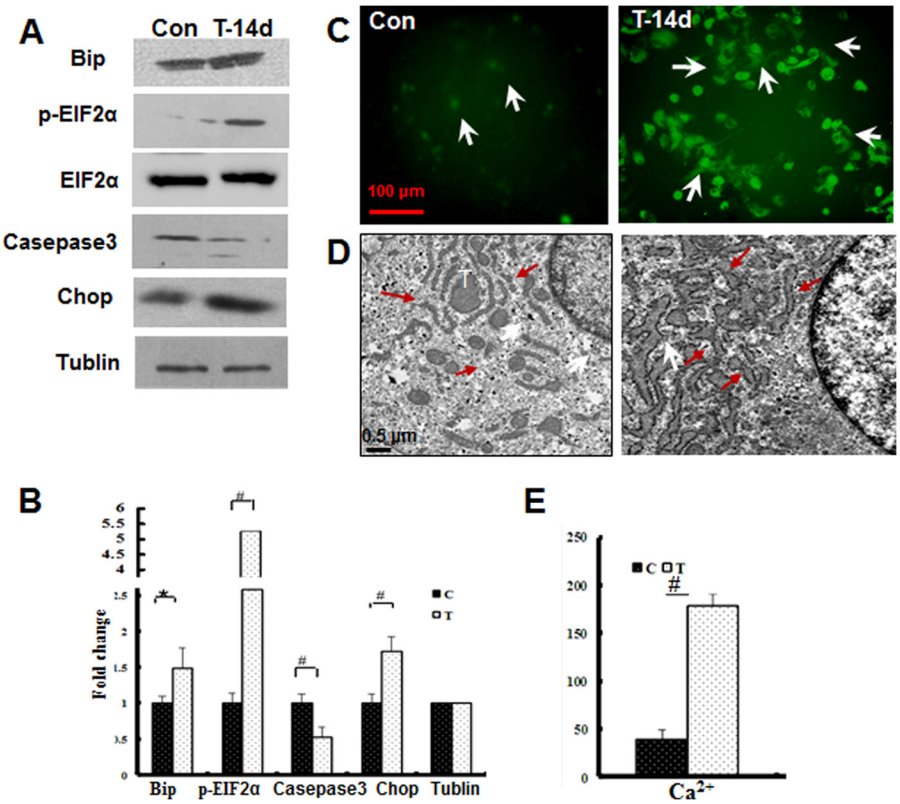

FIGURE 5. **Induction of ERS in response to mechanical stress.** *A*, Western blot analysis of the ERS marker proteins Bip, phospho-eIF2α, cleaved caspase-3, and CHOP from the control (*Con*) or mechanical stress-treated (*T-14d*) samples. *B*, quantification of the -fold changes in the proteins shown in *A* (#, $p < 0.01$; *, $p < 0.05$). *C*, effect of mechanical stress on free Ca^{2+} levels in mandibular chondrocytes as assessed by immunofluorescent staining. Free Ca^{2+} flux was visualized with a specific indicator (*white arrowhead*) (magnification ×100). *D*, TEM (magnification ×2000) revealed that the ER was expanded under mechanical stress (*red arrows*). *E*, the quantification of the changes in the Ca^{2+} levels is shown (#, $p < 0.01$). *Error bars*, S.D.

Previous studies have shown that ERS induces ER membrane expansion (25, 26). TEM analysis revealed that the ER membranes were expanded under mechanical stress (Fig. 5*D*), indicating that ERS occurred in these processes. These results provide direct evidence that ERS is induced upon mechanical stress treatment.

Mechanical Stress-induced Cell Cycle Arrest, Proliferation Inhibition, and Apoptosis as a Function of Loading Time—To explore the mechanisms underlying chondrocyte loss and cartilage thinning, we examined the occurrence of apoptosis and proliferation during mechanical stress loading. We examined apoptosis with the TUNEL assay. As shown in Fig. 6, *A* and *B*, dramatic cell death was observed at 3 days post-treatment. Positive staining was predominantly observed in the transitional and hypertrophic zone but not in the proliferative zone. Cell death was largely reduced in the samples at 7 and 14 days post-treatment. The effects of mechanical stress on chondrocyte proliferation were further examined. Cell cycle analysis by flow cytometry indicated that more cells were observed in the G_0/G_1 phase compared with the controls at 14 days post-treatment ($p < 0.01$) (Fig. 6, *C* and *D*), indicating inhibition of proliferation. Indeed, the expression of cyclin D1 was significantly reduced in isolated chondrocytes at 14 days post-treatment (Fig. 6*E*). Similarly, reduced cyclin D1 expression was observed in the cartilage during mechanical stress loading (Fig. 6, *F* and *G*). Furthermore, PCNA expression was reduced to 20% compared with the control group at 3 days, and this low level of expression remained at 7 and 14 days post-treatment (Fig. 6, *F* and *G*). These results indicated that the proliferation of mandibular cartilage was continuously inhibited during mechanical stress loading, whereas apoptosis occurred primarily during early loading. These changes provide an explanation for the observation of cartilage thinning after mechanical stress loading.

Inhibition of ERS Alleviates Mandibular Cartilage Thinning—ERS typically induces apoptosis and inhibits proliferation in many physiological and pathological processes (23, 24); therefore, we proposed that the induced apoptosis and proliferation inhibition observed under mechanical stress might reflect ERS. To test this hypothesis, we utilized an ERS-selective inhibitor, salubrinal, to examine the effects of ERS inhibition on the cartilage homeostasis response to mechanical stress. The efficiency of salubrinal treatment was confirmed in primary chondrocytes by Western blot analysis, as described previously in an *in vitro* ERS study (20, 27) (supplemental Fig. S4). In the present study, the histological analysis (Fig. 7, *A* and *B*) revealed that the thickness of the mandibular cartilage in the salubrinal/stressed group recovered, particularly in the hypertrophic zone, and the arrangement was more organized. The thinning mandibular cartilage was restored from one-third to two-thirds the thickness and the cell numbers of the control cartilage. However, reductions in the extracellular matrix and changes in the subchondral bone showed no significant recovery after salubrinal treatment (data not shown). TEM analysis revealed the resto-

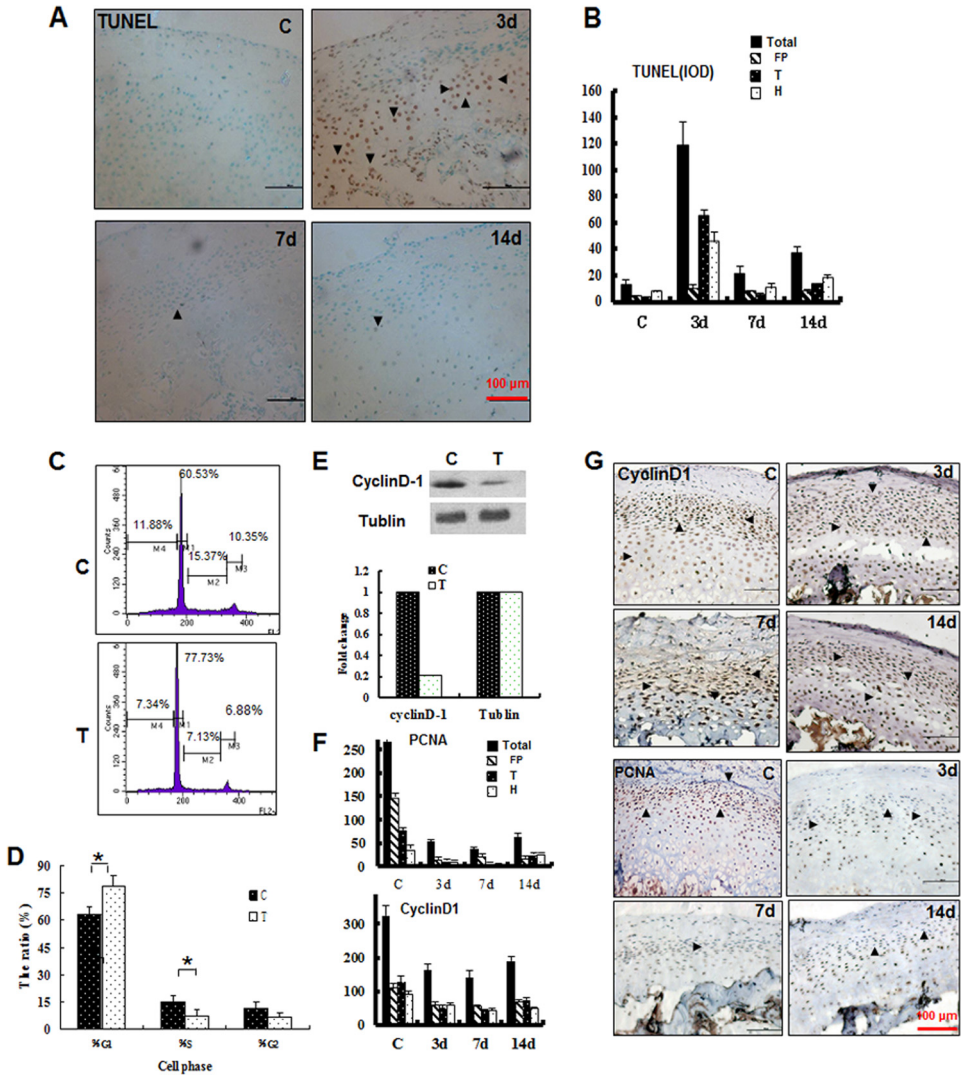

FIGURE 6. **Mechanical stress-induced apoptosis, cell cycle arrest, and proliferation inhibition at different loading times.** *A*, apoptosis was examined by TUNEL staining. *B*, quantification of *A* by integral optical density (*IOD*). *C*, cell cycle analysis of mandibular chondrocytes treated (*T*) or untreated (*C*) with mechanical stress for 14 days. *D*, the DNA histogram revealed a marked reduction in the S-phase percentage and increase in the G_1-phase percentage (*, $p < 0.05$). *E*, Western blot analysis of cyclin D1 expression and quantification of the changes in the samples treated (*T*) or untreated (*C*) with mechanical stress for 14 days. *F* and *G*, immunohistochemical analysis of PCNA and cyclin D1 in samples treated for the indicated number of days. *Error bars*, S.D.

ration of expanded ER membranes under mechanical stress after the inhibition of ERS (Fig. 7*C*).

Moreover, the inhibition of ERS by treatment with salubrinal significantly increased the expression of proliferative proteins, such as PCNA and Ki67, in the 14-day post-stress treatment samples obtained from the experimental group. The expression of PCNA and Ki67 was reduced to one-third and increased or recovered to two-thirds that of the control cartilage after salubrinal injection (Fig. 7, *D*, *E*, and *G*). The early apoptosis observed after mechanical stress for 3 days was significantly suppressed after salubrinal injection (Fig. 7, *F* and *G*). These results demonstrate that the inhibition of ERS regulates cartilage thinning through the induction of apoptosis and inhibition of proliferation and suggest that ERS plays an important role in pathogenesis under compressive mechanical stimulation.

DISCUSSION

Chondrocyte proliferation and the thickness of the mandibular cartilage are modulated by mechanical stimuli. Furthermore, many studies have indicated that cartilage thinning is important in the pathogenesis of TMJ diseases (14, 28–31). Teramoto *et al.* (14) demonstrated a significant decrease in the proliferation of condylar cartilage and the amount of extracellular matrix under compressive force, and we also previously demonstrated reduced proliferation of mandibular chondrocytes in response to mechanical stress *in vitro* (11). The results of the present study are consistent with these studies. In addition, the present study revealed the pathological change characterized by prominent cartilage thinning, reduced chondrocyte numbers, low proliferation, extracellular matrix degradation, and subchondral bone erosion (32, 33).

Mechanical force or physical stress has "nonspecific" effects on cells. Emerging studies have indicated that mechanical stress-induced specific cellular signaling, referred to as mechanotransduction, plays important roles in normal development and tissue dysfunction and degeneration. Although several cellular events, such as calcium oscillation and extracellular matrix and actin reorganization, have been identified during

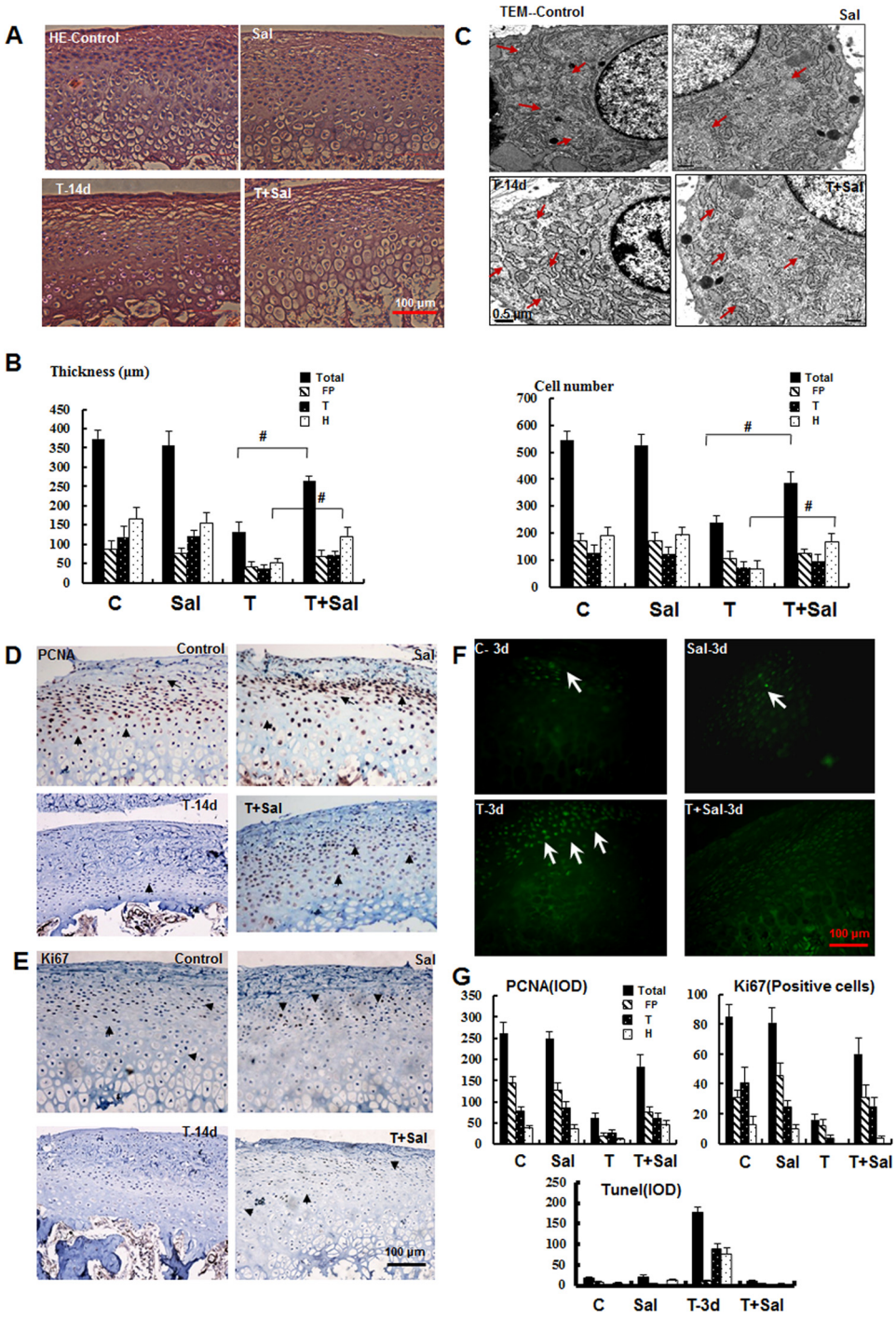

FIGURE 7. **Inhibition of ERS alleviates mandibular cartilage thinning.** *A*, H&E staining of the mandibular cartilage from samples treated as indicated for 14 days (magnification ×100). *Sal*, salubrinal. *B*, quantification of the results shown in *A* for the cartilage thickness and cell number in different zones as indicated (#, $p < 0.01$). *C*, TEM (magnification ×2000) revealed that the expanded ER membrane under mechanical stress was improved after inhibition of ERS (*red arrowhead*). *D* and *E*, immunohistochemical analysis of PCNA and Ki67 in samples treated for 14 days. *F*, TUNEL staining of samples treated as indicated for 3 days. *G*, quantification of the observed proliferation and apoptosis. *Error bars*, S.D.

mechanical stress, the specific molecular mechanisms underlying these processes, particularly mechanical stress-induced cell death, remain largely unknown. In the current study, we identified several candidate proteins, including PDI, CRT, TCTP, and Pin-1, that are involved in ERS and exhibit down-regulated protein or phosphorylation levels during mechanical stress treatment. Further examination by transmission electron microscopy indicated that ER membrane expansion occurs during stress treatment. These data indicate that ERS accompanied by severe cell death is induced in rat mandibular cartilage in response to mechanical force *in vivo*. Importantly, the application of an ERS-specific inhibitor efficiently suppressed cell death. ERS-induced apoptosis plays a critical role in the progression of neurodegenerative diseases. The data indicate that ERS-induced cell death also plays an important role in the mandibular cartilage thinning induced by mechanical stress.

Whether other apoptotic pathways are involved in mechanical stress-induced cell death remains unknown. Taken together, these data provide a novel mechanism for chondrocyte apoptosis induced by mechanical force and suggest a novel signaling target for mechanical stress.

These data also demonstrate that the isolated chondrocytes exhibited altered cell cycle progression during mechanical stress treatments. Indeed, previous studies have shown that eIF2α (translation elongation initiation factor 2α) inhibits the translation of cyclin D1, which in turn arrests cells in the G_1/S transition. Interestingly, the use of salubrinal, a specific inhibitor of eIF2α, in the present study restored the levels of Ki67 and PCNA in chondrocytes after mechanical stress treatment. These data suggest that eIF2α is a critical effector for the arrested cell cycle progression induced in chondrocytes by mechanical stress, implicating this effector as a pharmaceutical target for the study of mechanical stress-induced mandibular cartilage thinning.

Consistent with previous studies, these data also identified other candidates involved in cytoskeleton reorganization and cell metabolism during mechanical stress. It has been shown that TCTP expression is reduced in response to ER stress. Furthermore, the down-regulation of Pin-1 expression has also been observed under ER stress conditions. The data obtained in the present study also indicate that levels of TCTP expression and Pin-1 phosphorylation are reduced in response to mechanical stimuli. These data suggest other targets for ERS in chondrocytes that merit further study. Taken together, our data demonstrate that ERS is a critical intracellular target in mechanically stressed chondrocytes and indicate a novel role of ERS in mandibular cartilage thinning induced by mechanical stimuli.

Acknowledgments—We thank Prof. Qin-gang Hu, Prof. Wen-mei Wang, and Prof. Wei-bing Sun (Stomatological Hospital of Nanjing University) for giving support to this study.

REFERENCES

1. Sicher, H. (1947) The growth of the mandible. *Am. J. Orthod.* **43,** 123–128
2. Kiliaridis, S., Thilander, B., Kjellberg, H., Topouzelis, N., and Zafiriadis, A. (1999) Effect of low masticatory function on condylar growth. A morphometric study in the rat. *Am. J. Orthod. Dentofacial Orthop.* **116,** 121–125
3. Murray, R. C., Zhu, C. F., Goodship, A. E., Lakhani, K. H., Agrawal, C. M., and Athanasiou, K. A. (1999) Exercise affects the mechanical properties and histological appearance of equine articular cartilage. *J. Orthop. Res.* **17,** 725–731
4. Kuroda, S., Tanimoto, K., Izawa, T., Fujihara, S., Koolstra, J. H., and Tanaka, E. (2009) Biomechanical and biochemical characteristics of the mandibular condylar cartilage. *Osteoarthr. Cartil.* **17,** 1408–1415
5. Wadhwa, S., and Kapila, S. (2008) TMJ disorders. Future innovations in diagnostics and therapeutics. *J. Dent. Educ.* **72,** 930–947
6. Millward-Sadler, S. J., Wright, M. O., Lee, H., Nishida, K., Caldwell, H., Nuki, G., and Salter, D. M. (1999) Integrin-regulated secretion of interleukin 4. A novel pathway of mechanotransduction in human articular chondrocytes. *J. Cell Biol.* **145,** 183–189
7. Roberts, S. R., Knight, M. M., Lee, D. A., and Bader, D. L. (2001) Mechanical compression influences intracellular Ca^{2+} signaling in chondrocytes seeded in agarose constructs. *J. Appl. Physiol.* **90,** 1385–1391
8. Takebe, K., Nishiyama, T., Hayashi, S., Hashimoto, S., Fujishiro, T., Kanzaki, N., Kawakita, K., Iwasa, K., Kuroda, R., and Kurosaka, M. (2011) Regulation of p38 MAPK phosphorylation inhibits chondrocyte apoptosis in response to heat stress or mechanical stress. *Int. J. Mol. Med.* **27,** 329–335
9. Hermansson, M., Sawaji, Y., Bolton, M., Alexander, S., Wallace, A., Begum, S., Wait, R., and Saklatvala, J. (2004) Proteomic analysis of articular cartilage shows increased type II collagen synthesis in osteoarthritis and expression of inhibin βA (activin A), a regulatory molecule for chondrocytes. *J. Biol. Chem.* **279,** 43514–43521
10. Ruiz-Romero, C., López-Armada, M. J., and Blanco, F. J. (2005) Proteomic characterization of human normal articular chondrocytes. A novel tool for the study of osteoarthritis and other rheumatic diseases. *Proteomics* **5,** 3048–3059
11. Li, H., Yang, H. S., Wu, T. J., Zhang, X. Y., Jiang, W. H., Ma, Q. L., Chen, Y. X., Xu, Y., Li, S., and Hua, Z. C. (2010) Proteomic analysis of early-response to mechanical stress in neonatal ratmandibular condylar chondrocytes. *J. Cell Physiol.* **223,** 610–622
12. Miki, T., and Yamamuro, T. (1987) The fate of hypertrophic chondrocytes in growth plates transplanted intramuscularly in the rabbit. *Clin. Orthop. Relat. Res.* **218,** 276–282
13. Habib, H., Hatta, T., Udagawa, J., Zhang, L., Yoshimura, Y., and Otani, H. (2005) Fetal jaw movement affects condylar cartilage development. *J. Dent. Res.* **84,** 474–479
14. Teramoto, M., Kaneko, S., Shibata, S., Yanagishita, M., and Soma, K. (2003) Effect of compressive forces on extracellular matrix in rat mandibular condylar cartilage. *J. Bone Miner. Metab.* **21,** 276–286
15. Mizoguchi, I., Takahashi, I., Nakamura, M., Sasano, Y., Sato, S., Kagayama, M., and Mitani, H. (1996) An immunohistochemical study of regional differences in the distribution of type I and type II collagens in rat mandibular condylar cartilage. *Arch. Oral Biol.* **41,** 863–869
16. Kronfeld, K., Hochleitner, E., Mendler, S., Goldschmidt, J., Lichtenfels, R., Lottspeich, F., Abken, H., and Seliger, B. (2005) B7/CD28 costimulation of T cells induces a distinct proteome pattern. *Mol. Cell Proteomics* **4,** 1876–1887
17. Yu, L. R., Zeng, R., Shao, X. X., Wang, N., Xu, Y. H., and Xia, Q. C. (2000) Identification of differentially expressed proteins between human hepatoma and normal liver cell lines by two-dimensional electrophoresis and liquid chromatography-ion trap mass spectrometry. *Electrophoresis* **21,** 3058–3068
18. Yang, W., Liu, P., Liu, Y., Wang, Q., Tong, Y., and Ji, J. (2006) Proteomic analysis of rat pheochromocytoma PC12 cells. *Proteomics* **6,** 2982–2990
19. Gobom, J., Schuerenberg, M., Mueller, M., Theiss, D., Lehrach, H., and Nordhoff, E. (2001) α-Cyano-4-hydroxycinnamic acid affinity sample preparation. A protocol for MALDI-MS peptide analysis in proteomics. *Anal. Chem.* **73,** 434–438
20. Sohen, S., Ooe, H., Hashima, M., Nonaka, T., Fukuda, K., and Hamanishi, C. (2001) Activation of histamine H1 receptor results in enhanced proteoglycan synthesis by human articular chondrocyte. Involvement of protein kinase C and intracellular Ca^{2+}. *Pathophysiology* **8,** 93–98
21. Sokka, A. L., Putkonen, N., Mudo, G., Pryazhnikov, E., Reijonen, S., Khiroug, L., Belluardo, N., Lindholm, D., and Korhonen, L. (2007) Endoplasmic reticulum stress inhibition protects against excitotoxic neuronal injury in the rat brain. *J. Neurosci.* **27,** 901–908
22. Suzuki, S., Itoh, K., and Ohyama, K. (2004) Local administration of IGF-I stimulates the growth of mandibular condyle inmature rats. *J. Orthod.* **31,** 138–143
23. Wang, X. Z., Lawson, B., Brewer, J. W., Zinszner, H., Sanjay, A., Mi, L. J., Boorstein, R., Kreibich, G., Hendershot, L. M., and Ron, D. (1996) Signals from the stressed endoplasmic reticulum induce C/EBP-homologous protein (CHOP/GADD153). *Mol. Cell. Biol.* **16,** 4273–4280
24. Schröder, M. (2008) Endoplasmic reticulum stress responses. *Cell Mol. Life Sci.* **65,** 862–894
25. Shaffer, A. L., Shapiro-Shelef, M., Iwakoshi, N. N., Lee, A. H., Qian, S. B., Zhao, H., Yu, X., Yang, L., Tan, B. K., Rosenwald, A., Hurt, E. M., Petroulakis, E., Sonenberg, N., Yewdell, J. W., Calame, K., Glimcher, L. H., and Staudt, L. M. (2004) XBP1, downstream of Blimp-1, expands the secretory apparatus and other organelles, and increases protein synthesis in plasma cell differentiation. *Immunity* **21,** 81–93
26. Sriburi, R., Jackowski, S., Mori, K., and Brewer, J. W. (2004) XBP1. A link between the unfolded protein response, lipid biosynthesis, and biogenesis

of the endoplasmic reticulum. *J. Cell Biol.* **167,** 35–41
27. Boyce, M., Bryant, K. F., Jousse, C., Long, K., Harding, H. P., Scheuner, D., Kaufman, R. J., Ma, D., Coen, D. M., Ron, D., and Yuan, J. (2005) A selective inhibitor of eIF2α dephosphorylation protects cells from ER stress. *Science* **307,** 935–939
28. Copray, J. C., Jansen, H. W., and Duterloo, H. S. (1985) An *in vitro* system for studying the effect of variable compressive forces on mandibular condylar cartilage of the rat. *Arch. Oral Biol.* **30,** 305–311
29. Lee, J. H., Fitzgerald, J. B., Dimicco, M. A., and Grodzinsky, A. J. (2005) Mechanical injury of cartilage explants causes specific time-dependent changes inchondrocyte gene expression. *Arthritis Rheum.* **52,** 2386–2395
30. Sriram, D., Jones, A., Alatli-Burt, I., and Darendeliler, M. A. (2009) Effects of mechanical stimuli on adaptive remodeling of condylar cartilage. *J. Dent. Res.* **88,** 466–470
31. Tasci, A., Ferguson, S. J., and Büchler, P. (2011) Numerical assessment on the effective mechanical stimuli for matrix-associated metabolism in chondrocyte-seeded constructs. *J. Tissue Eng. Regen. Med.* **5,** 210–219
32. Embree, M., Ono, M., Kilts, T., Walker, D., Langguth, J., Mao, J., Bi, Y., Barth, J. L., and Young, M. (2011) Role of subchondral bone during early-stage experimental TMJ osteoarthritis. *J. Dent. Res.* **90,** 1331–1338
33. Jiao, K., Niu, L. N., Wang, M. Q., Dai, J., Yu, S. B., Liu, X. D., and Wang, J. (2011) Subchondral bone loss following orthodontically induced cartilage degradation in the mandibular condyles of rats. *Bone* **48,** 362–371